


# Electron states in a sinusoidally deformed cylindrical quantum wire

Moletlanyi Tshipa<sup>1</sup> 

Received: 31 December 2016 / Accepted: 11 March 2017 / Published online: 25 March 2017  
© The Author(s) 2017. This article is an open access publication

**Abstract** Electron states in a sinusoidally deformed cylindrical nanowire are probed within the effective mass approximation. The nanowire is immersed in a homogeneous magnetic field applied parallel to the axis of the wire. The sinusoidal deformity affects quantum properties of electrons considerably. The deformity introduces energy dependence on the axial position, enhancing (decreasing) confinement energies in regions where the radius is narrower (wider). Analysis shows that the magnetic field attenuates these sinusoidal deformity-induced distortions on electron quantum properties

**Keywords** Electron states · Nanowire · Magnetic field · Electron confinement

**Mathematics Subject Classification** 81S10

## Introduction

Recent advances in nanotechnology have made it possible to fabricate nanowires of different sizes and geometries [1–4]. Nanowires have a variety of novel properties, rendering them invaluable in diverse disciplines like medicine [5], optoelectronics [6] and energy physics [7], among others. However, due to the small dimensions concerned, it is very difficult to fabricate nanostructures with controllable and uniform cross-sectional area, to which some effort has been directed [8]. Apart from the difficulty in

fabricating nanowires of uniform cross-sectional area, it may be beneficial to produce nanowires with non-uniform cross-sectional area [9–12].

Most of the operational principles of nanodevices rest on the nature of quantum states in nanostructures. A better understanding of quantum states in various systems, therefore, is imperative [13, 14]. Thus, the main endeavour of this communication is to interrogate the effect of deformities of cylindrical nanowires on quantum states of electrons in such nanostructures. This communication is arranged as follows. Section 2 deals with the theoretical underpinnings for the system. The pertaining results are found in Sect. 3, with the conclusions laid in Sect. 4.

## Theoretical framework

The envisaged system is a cylindrical quantum wire of height  $L_z$ , whose radius  $R(z)$  depends sinusoidally on the axial position of the nanowire. The wire is immersed in an external magnetic field  $\mathbf{B}$  directed axially, obtainable from the vector potential taken in the gauge  $\mathbf{A} = (0, \frac{1}{2}\mathbf{B}\rho, 0)$ . Due to the cylindrical symmetry of the system, the time-independent electron wave function can be expressed as  $\Psi(\rho, z, \phi) = C_{lmn}\chi(\rho) \sin(n\pi z/L_z)e^{im\phi}$ , where  $C_{lmn}$  is the normalization constant and  $\chi(\rho)$  is the radial component of the wave function satisfying the Schrödinger equation

$$\frac{1}{\rho} \frac{d}{d\rho} \left( \rho \frac{d}{d\rho} \chi(\rho) \right) + \left\{ \frac{2\mu}{\hbar^2} [\Xi_{ml} - V(\rho, z) - U_B] - \frac{|m|^2}{\rho^2} \right\} \chi(\rho) = 0 \quad (1)$$

with  $\Xi_{ml} = E_{ml} - \frac{1}{2}m\hbar\omega_c$  and  $U_B = \frac{1}{8}\mu\omega_c^2\rho^2$ ,  $\omega_c = eB/\mu$  being the cyclotron frequency. The electron effective mass is denoted by  $\mu$  while  $V(\rho, z) = V(\rho)V(z)$  is the confining

✉ Moletlanyi Tshipa  
tshipam@mopipi.ub.bw

<sup>1</sup> University of Botswana, Private Bag 0022, Gaborone, Botswana

electric potential. Here,  $\hbar$  is the reduced Planck’s constant,  $n$  the axial principal quantum number and  $m$  is the azimuthal quantum number that quantifies the angular momentum of an electron.

The electric potential for this nanowire is modelled as

$$V(\rho, z) = \begin{cases} 0 & \dots \rho < R(z) \cup 0 < z < L_z \\ \infty & \dots \rho > R(z) \cup -\infty < z < 0 \cup z > L_z \end{cases}$$

where  $R(z)$  is given by

$$R(z) = R_0 \left\{ 1 + \alpha(z/L_z)^\beta \left[ 1 + \sin\left(\frac{N\pi z}{L_z}\right) \right] \right\}, \tag{2}$$

where  $\alpha$  quantifies the degree of sinusoidal deformity and  $\beta$  determines the envelope profile of the sinusoidal deformity across the length of the wire.  $N$  is a positive real number, which for this communication has been taken as an integer.  $R_0$  plays the role of the minimum radius that the wire can have anywhere along its length.

The radial part of the Schrödinger equation is solvable in terms of the hypergeometric function;

$$\chi(\rho) = e^{-\varsigma/2} (\varsigma)^{b/2} M(a, b, \varsigma) \tag{3}$$

with

$$\begin{aligned} \varsigma &= \frac{\mu\omega_c}{2\hbar} \rho^2, \\ a &= \frac{1+m}{2} - \frac{E_{ml} - \frac{1}{2}m\hbar\omega_c}{\hbar\omega_c}, \\ b &= 1+m \end{aligned}$$

and

$$\varsigma = \frac{\mu\omega_c}{2\hbar} \rho^2.$$

The energy spectrum is obtainable from the usual boundary conditions at the walls of the nanowire as

$$E_{ml} = \left( \frac{1+m}{2} - a_0 \right) \hbar\omega_c + \frac{1}{2}m\hbar\omega_c \tag{4}$$

where  $a_0$  satisfies the condition  $M(a_0, b, \varsigma_R) = 0$ , with  $\varsigma_R = \frac{\mu\omega_c}{2\hbar} R(z)^2$ .

### Results and discussions

The effective mass used in this work pertains to GaAs nanowires:  $\mu = 0.067m_e$ ,  $m_e$  being the free electron mass. The geometry of the nanowires can be viewed in Fig. 1, where only the  $N = 6$  case has been illustrated. In this figure, the effect of the envelope profile of the sinusoidal deformity,  $\beta$ , on the geometry of the wires can also be viewed, which has been taken to be linear ( $\beta = 1$ ). Even though it is possible for  $\beta$  to assume negative values, for

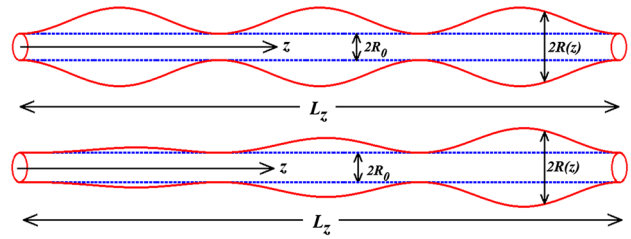


**Fig. 1** Schematic representation of the sinusoidally deformed nanowire, for  $N = 6$ . The upper wire is for  $\beta = 0$  while the lower is for  $\beta = 1$

this communication, we shall restrict  $\beta$  only to positive values.

For integer  $N$ , the radius of the wire has  $\{\frac{N+1}{2}, \frac{N+1}{2}\}$  points of minimum and maximum values for odd  $N$ , and  $\{\frac{N+2}{2}, \frac{N}{2}\}$  for even  $N$ , where  $\{N_{R_{min}}, N_{R_{max}}\}$  represents the number of points where the radius is minimum ( $R_{min} = R_0$ ) and maximum ( $R_{max}$ ), respectively. Consequently, for sinusoidally deformed cylindrical wires, the electron wave functions are diminished (enhanced) in regions where  $R = R_{min}$  ( $R = R_{max}$ ) as the axial position is swept (Fig. 2).

Figure 3 shows the effect of the  $\beta$  parameter on the  $n = 2$  electron wave functions. For non-zero  $\beta$ , one side of the wire is larger than the other, hence the electron wave functions in regions where the nanowire is smaller (wider) become diminished (enhanced). This is a consequence of the fact that it requires larger energies to occupy a narrower region than a larger one.

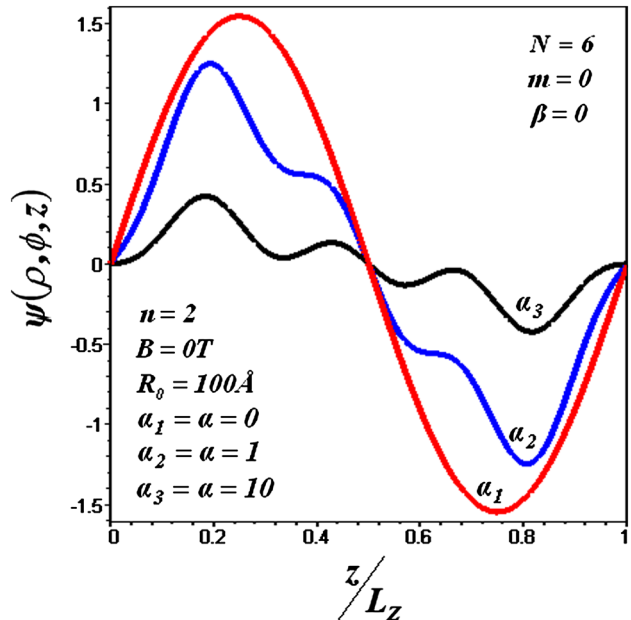


**Fig. 2** The variation of the electron wave function with the axial position in a sinusoidally deformed quantum wire (for  $N = 6$ ,  $n = 2$ ) for the different  $\alpha$  values

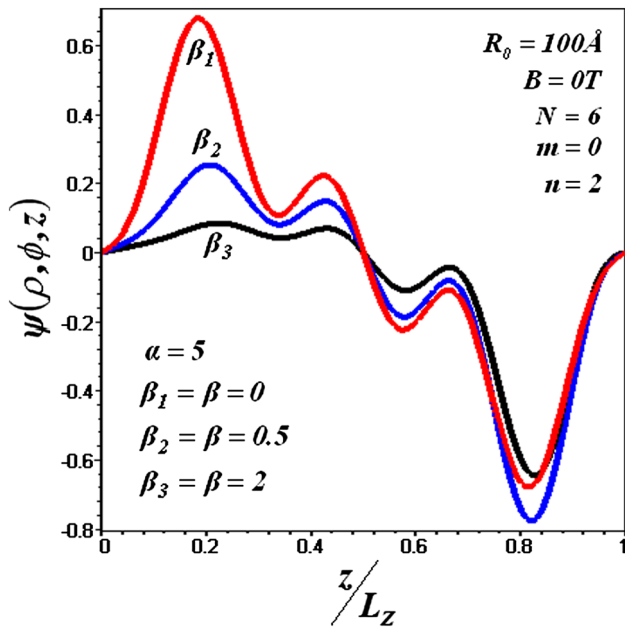


**Fig. 3** The effect of  $\beta$  on the wave function as a function of the axial position (also for  $N = 6, n = 2$ )

As functions of the axial position, the energy eigenvalues are characterised by oscillations of enhancement and decrement, corresponding to increased radial confinement and relaxation, respectively (Fig. 4). For  $\beta = 0$ , the energies at  $z = 0$  equal those at  $z = L_z$  for nanowires with even  $N$  sinusoidal deformation. For odd  $N$ , the energies at  $z = L_z$  are always less than those at  $z = 0$ , since the radius at  $z = L_z$  is greater than at  $z = 0$ . For  $\beta \neq 0$ , the energies at

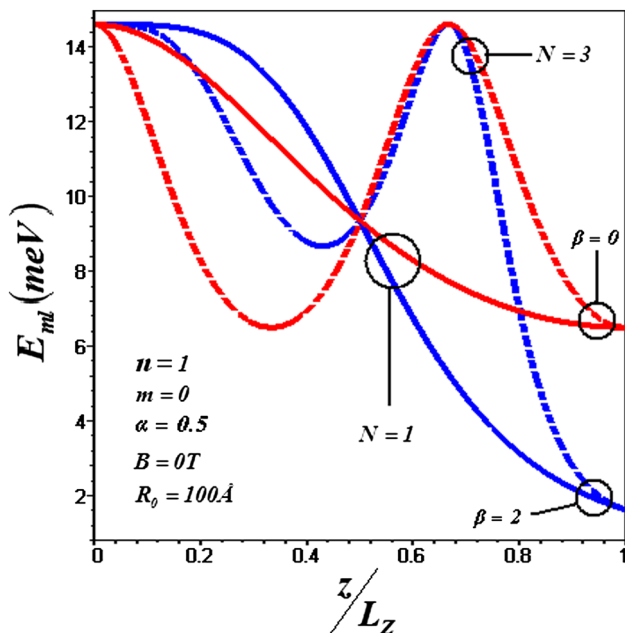


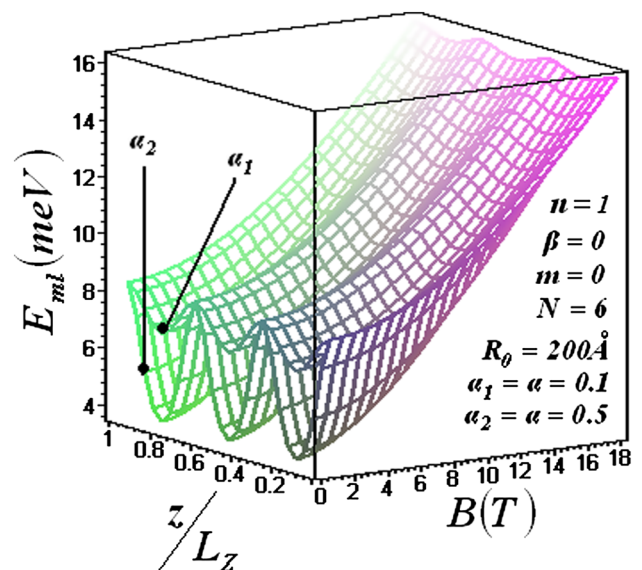
**Fig. 4** The effect of  $\beta$  on the radial confinement energies as functions of the axial position for  $N = 1$  and  $N = 3$

$z = L_z$  are always lower than those at  $z = 0$ , since in this case the latter portion ( $z = 0$ ) is smaller than the former ( $z = L_z$ ), both for even and odd  $N$ .

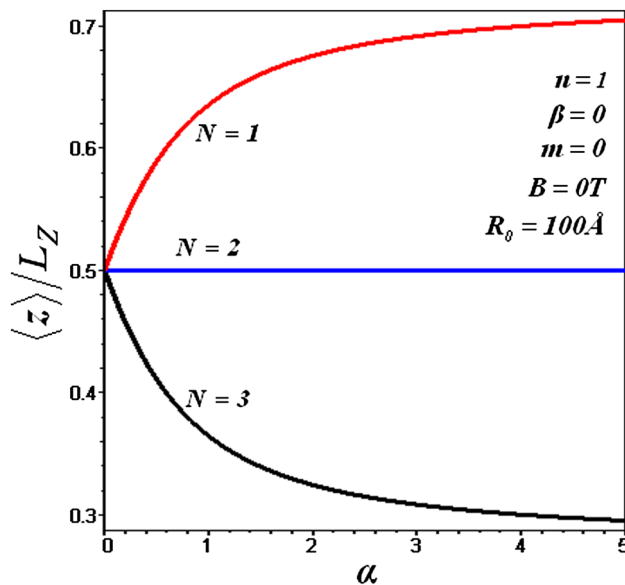
Since the azimuthal quantum number  $m$  quantifies angular momenta of different states, the radial expectation values of electrons with higher  $m$  values are greater than those with lower  $m$  values. This makes the higher  $m$  valued states to be more susceptible to the variation in the size of the radius. Consequently, the energy dependence on the axial position for excited states has the same variation as those for the ground state, albeit more pronounced.

Figure 5 illustrates the change in variation of the radial confinement energy across the length of the nanowire (depicted in Fig. 1) as the magnetic field strength is increased. In the absence of the magnetic field, the sinusoidal deformity affects the radial confinement energies drastically. The magnetic field has the proclivity to lessen the effects of the sinusoidal deformity. This springs from the fact that the magnetic field increases confinement around the axis as it intensifies, reducing the effect of the walls of the nanostructure as the dominant confining factor.

Figure 6 depicts the dependence of the axial position expectation value  $\langle z \rangle$  on the degree of sinusoidal deformity  $\alpha$ . For a perfectly cylindrical nanowire, the axial position expectation value is at  $\langle z \rangle = 0.5L_z$ . When  $N = 1 + 4p, p = 0, 1, 2, 3, \dots$  (for example,  $N = 1$ ), as  $\alpha$  increases, one end of the nanowire becomes wider. The wider end is preferred by the electron because of low energies associated with it. This leads to enhancement of  $\langle z \rangle$  as  $\alpha$  increases. When  $N$  is even, however, increase in  $\alpha$  does not affect  $\langle z \rangle$  as regions on both sides of  $z = 0.5L_z$  (i.e.,  $z > 0.5L_z$  and  $z < 0.5L_z$ ) get identically sinusoidally deformed, resulting in no side



**Fig. 5** The dependence of the energy eigenvalues on the magnetic field strength across the length of the wire for the indicated values of  $\alpha$



**Fig. 6** The variation of the most probable axial position value with the degree of sinusoidal deformity  $\alpha$  for  $N = 1$ ,  $N = 2$  and  $N = 3$  in the absence of the magnetic field

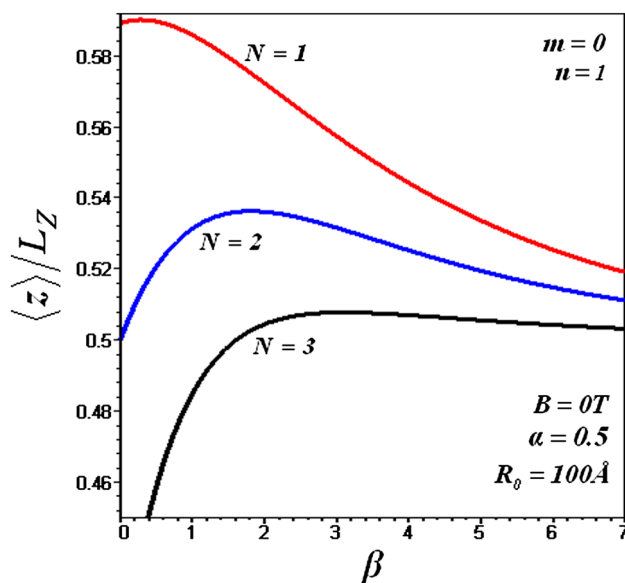


**Fig. 7** The effect of  $\beta$  on the most probable axial position for  $N = 1$ ,  $N = 2$  and  $N = 3$  in the absence of the magnetic field

( $z > 0.5L_Z$  or  $z < 0.5L_Z$ ) being preferred over the other. For nanowires with  $N = 3 + 4p$ ,  $p = 0, 1, 2, 3, \dots$  (for example  $N = 3$ ), the lower portion of the wire is relatively wider than the upper. This shifts electron wave functions towards the lower portion, reducing  $\langle z \rangle$ .

The effect of the axial profile of the sinusoidal deformity ( $\beta$ ) on the most probable axial position is depicted in Fig. 7. As  $\beta$  increases, the lower portion of the nanostructure becomes narrower than the upper. This displaces

the electron from the narrower lower portion, enhancing the axial expectation value. As  $\beta$  increases further, only a small portion of the nanowire is wider, at the topmost part. This reduces preference in that region, signified by the reduction of the axial expectation value as  $\beta$  further increases.

## Conclusions

Electron states in a sinusoidally deformed nanowire have been obtained through the effective mass approach. The effects of the sinusoidal deformity and the envelope profile of the deformity on quantum properties (wave functions, energy eigen values, position expectation values) have been investigated. The sinusoidal deformity merely compresses and decompresses the wave function across the length of the nanowire. This corresponds to modulation in electron energy eigen values. Additionally, the deformity increases the axial expectation value of electrons in nanowires with  $N = 1 + 4p$  and decreases that of electrons in nanowires with  $N = 3 + 4p$ , where  $p = 0, 1, 2, 3, \dots$ , while those of electrons in nanowires with even  $N$  remain unchanged only for  $\beta = 0$ .

**Open Access** This article is distributed under the terms of the Creative Commons Attribution 4.0 International License (<http://creativecommons.org/licenses/by/4.0/>), which permits unrestricted use, distribution, and reproduction in any medium, provided you give appropriate credit to the original author(s) and the source, provide a link to the Creative Commons license, and indicate if changes were made.

## References

- Koleva, M.E., Dutta, M., Fukata, N.: Mater. Sci. Eng. B **187**, 102 (2014). doi:10.1016/j.mseb.2014.05.008
- Toan, L.D., Moyen, E., Zamfir, M.R., Joe, J., Kim, Y.W., Pribat, D.: Mater. Res. Express **3**, 015003 (2016). doi:10.1088/2053-1591/3/1/015003
- Ivanov, Y.P., Chuvilin, A., Vivas, L.G., Kosel, J., Chubykalo-Fesenko, O., Vázquez, M.: Sci. Rep. **6**, 23844 (2016). doi:10.1038/srep23844
- Rishinaramangalam, A.K., Nami, M., Fairchild, M.N., Shima, D.M., Balakrishnan, G., Brueck, S.R.J., Feezell, D.F.: Appl. Phys. Express **9**, 032101 (2016). doi:10.7567/APEX.9.032101
- Wang, Z., Lee, S., Koo, K., Kim, K.: Trans. IEEE Nanobiosci **15**(3), 186 (2016). doi:10.1109/TNB.2016.2528258
- Wang, Z., Nabet, B.: Nanophotonics **4**, 491 (2015). doi:10.1515/nanoph-2015-0025
- Pathirane, M., Iheanacho, B., Tamang, A., Lee, C.H., Lujan, R., Knipp, D., Wong, W.S.: Appl. Phys. Lett. **107**, 143903 (2015). doi:10.1063/1.4932649
- Yang, Z.X., Han, N., Fang, M., Lin, H., Cheung, H.Y., Yip, S., Wang, E.J., Hung, T., Wong, C.Y., Ho, J.C.: Nat. Commun. **5**, 5249 (2014). doi:10.1038/ncomms6249
- Wang, N., Cai, Y., Zhang, R.Q.: Mater. Sci. Eng. R **60**, 1 (2008). doi:10.1016/j.mser.2008.01.001



10. Li, H., Shen, L., Ding, B., Pang, G., Dou, H., Zhang, X.: *Nano Energy* **13**, 18 (2015). doi:[10.1016/j.nanoen.2015.02.002](https://doi.org/10.1016/j.nanoen.2015.02.002)
11. Li, C., Zhao, L., Mao, Y., Wu, W., Xu, J.: *Sci. Rep.* **5**, 8236 (2015). doi:[10.1038/srep08236](https://doi.org/10.1038/srep08236)
12. Fernández-Domínguez, A.I., Martín-Moreno, L., García-Vidal, F.J., Andrews, S.R., Maier, S.A.: *IEEE J. Sel. Top. Quantum Electron.* **14**(6), 1515 (2008). doi:[10.1109/JSTQE.2008.918107](https://doi.org/10.1109/JSTQE.2008.918107)
13. Shi, Z., Simmons, C.B., Ward, D.R., Prance, J.R., Wu, X., Koh, T.S., Gamble, J.K., Seavage, D.E., Lagally, M.G., Friesen, M., Coppersmith, S.N., Eriksson, M.A.: *Nat. Commun.* **5**, 3020 (2014). doi:[10.1038/ncomms4020](https://doi.org/10.1038/ncomms4020)
14. Kazaryan, E.M., Petrosyan, L.S., Shahnazaryan, V.A., Sarkisyan, H.A.: *Commun. Theor. Phys.* **63**(2), 255 (2015)

